Ultrathin 90-degree sharp bends for spoof surface plasmon polaritons

Yang, Yihao; Chen, Hongsheng; Xiao, Sanshui ; Mortensen, N. Asger; Zhang, Jingjing

Published in:
Optics Express

Link to article, DOI:
10.1364/OE.23.019074

Publication date:
2015

Document Version
Publisher's PDF, also known as Version of record

Ultrathin 90-degree sharp bends for spoof surface plasmon polaritons

Yihao Yang,[1,2] Hongsheng Chen,[1] Sanshui Xiao,[2] N. Asger Mortensen,[2] and Jingjing Zhang[2,*]

[1]*Department of Information Science & Electronic Engineering, Zhejiang University, China*
[2] *Department of Photonics Engineering - DTU Fotonik, Technical University of Denmark, DK-2800 Kgs. Lyngby, Denmark*
**jinz@fotonik.dtu.dk*

Abstract: At low frequencies outside the plasmonic range, strongly confined surface waves can be achieved on periodically structured metal surfaces, thereby allowing for the design of compact electromagnetic guiding devices. Here, we propose an approach to realize highly efficient transmission of spoof surface plasmons around 90-degree sharp bends on ultrathin metallic films in the microwave regime. We demonstrate that by judiciously engineering the structure, the dispersion relation can be designed to reduce the scattering. Furthermore, the reflection can be suppressed by proper structural decoration at the bending corner. A one-dimensional scattering theory is employed to understand and verify the transmission properties of our waveguide bend structure. Our design scheme is not restricted to the specific structure we propose here but can be applied to other guiding components built up on two dimensional metal surfaces.

OCIS codes: (250.5403) Plasmonics; (160.3918) Metamaterials; (240.6690) Surface waves.

References and links

1. W. L. Barnes, A. Dereux, and T. W. Ebbesen, "Surface plasmon subwavelength optics," Nature **424**(6950), 824–830 (2003).
2. W. H. Tsai, Y. C. Tsao, H. Y. Lin, and B. C. Sheu, "Cross-point analysis for a multimode fiber sensor based on surface plasmon resonance," Opt. Lett. **30**(17), 2209–2211 (2005).
3. M. L. Brongersma and V. M. Shalaev, "Applied physics. The case for plasmonics," Science **328**(5977), 440–441 (2010).
4. J. Zhang, S. Xiao, M. Wubs, and N. A. Mortensen, "Surface plasmon wave adapter designed with transformation optics," ACS Nano **5**(6), 4359–4364 (2011).
5. Y. Luo, A. Aubry, and J. B. Pendry, "Electromagnetic contribution to surface-enhanced Raman scattering from rough metal surfaces: a transformation optics approach," Phys. Rev. B **83**(15), 155422 (2011).
6. Y. Luo, J. B. Pendry, and A. Aubry, "Surface plasmons and singularities," Nano Lett. **10**(10), 4186–4191 (2010).
7. P. Andrew, S. C. Kitson, and W. L. Barnes, "Surface-plasmon energy gaps and photoabsorption," J. Mod. Opt. **44**(2), 395–406 (1997).
8. J. L. Coutaz, M. Neviere, E. Pic, and R. Reinisch, "Experimental study of surface-enhanced second-harmonic generation on silver gratings," Phys. Rev. B Condens. Matter **32**(4), 2227–2232 (1985).
9. Y. Luo, D. Y. Lei, S. A. Maier, and J. B. Pendry, "Broadband light harvesting nanostructures robust to edge bluntness," Phys. Rev. Lett. **108**(2), 023901 (2012).
10. J. B. Pendry, A. I. Fernandez-Dominguez, Y. Luo, and R. Zhao, "Capturing photons with transformation optics," Nat. Phys. **9**(8), 518–522 (2013).
11. Y. Luo, D. Y. Lei, S. A. Maier, and J. B. Pendry, "Transformation-optics description of plasmonic nanostructures containing blunt edges/corners: from symmetric to asymmetric edge rounding," ACS Nano **6**(7), 6492–6506 (2012).
12. J. B. Pendry, Y. Luo, and R. Zhao, "Transforming the optical landscape," Science **348**(6234), 521–524 (2015).
13. Y. Luo, R. Zhao, and J. B. Pendry, "van der Waals interactions at the nanoscale: the effects of nonlocality," Proc. Natl. Acad. Sci. U.S.A. **111**(52), 18422–18427 (2014).
14. J. B. Pendry, L. Martín-Moreno, and F. J. Garcia-Vidal, "Mimicking surface plasmons with structured surfaces," Science **305**(5685), 847–848 (2004).

#241242 Received 18 May 2015; revised 29 Jun 2015; accepted 13 Jul 2015; published 15 Jul 2015

15. J. J. Wood, L. A. Tomlinson, O. Hess, S. A. Maier, and A. I. Fernández-Domínguez, "Spoof plasmon polaritons in slanted geometries," Phys. Rev. B **85**(7), 075441 (2012).
16. F. J. Garcia-Vidal, L. Martin-Moreno, and J. B. Pendry, "Surfaces with holes in them: new plasmonic metamaterials," J. Opt. A, Pure Appl. Opt. **7**(2), S97–S101 (2005).
17. D. Martin-Cano, M. L. Nesterov, A. I. Fernandez-Dominguez, F. J. Garcia-Vidal, L. Martin-Moreno, and E. Moreno, "Domino plasmons for subwavelength terahertz circuitry," Opt. Express **18**(2), 754–764 (2010).
18. Y. G. Ma, L. Lan, S. M. Zhong, and C. K. Ong, "Experimental demonstration of subwavelength domino plasmon devices for compact high-frequency circuit," Opt. Express **19**(22), 21189–21198 (2011).
19. A. I. Fernández-Domínguez, L. Martín-Moreno, F. J. García-Vidal, S. R. Andrews, and S. A. Maier, "Spoof surface plasmon polariton modes propagating along periodically corrugated wires," IEEE. J. Sel. Top. Quantum Electron. **14**(6), 1515–1521 (2008).
20. S. A. Maier, S. R. Andrews, L. Martín-Moreno, and F. J. García-Vidal, "Terahertz surface plasmon-polariton propagation and focusing on periodically corrugated metal wires," Phys. Rev. Lett. **97**(17), 176805 (2006).
21. M. Navarro-Cía, M. Beruete, S. Agrafiotis, F. Falcone, M. Sorolla, and S. A. Maier, "Broadband spoof plasmons and subwavelength electromagnetic energy confinement on ultrathin metafilms," Opt. Express **17**(20), 18184–18195 (2009).
22. X. Shen, T. J. Cui, D. Martin-Cano, and F. J. Garcia-Vidal, "Conformal surface plasmons propagating on ultrathin and flexible films," Proc. Natl. Acad. Sci. U.S.A. **110**(1), 40–45 (2013).
23. Z. Liao, Y. Luo, A. I. Fernández-Domínguez, X. Shen, S. A. Maier, and T. J. Cui, "High-order localized spoof surface plasmon resonances and experimental verifications," Sci. Rep. **5**, 9590 (2015).
24. H. C. Zhang, S. Liu, X. Shen, L. H. Chen, L. Li, and T. J. Cui, "Broadband amplification of spoof surface plasmon polaritons at microwave frequencies," Laser Photonics Rev. **9**(1), 83–90 (2015).
25. X. Wan, X. Shen, Y. Luo, and T. J. Cui, "Planar bifunctional Luneburg-fisheye lens made of an anisotropic metasurface," Laser Photonics Rev. **8**(5), 757–765 (2014).
26. J. J. Xu, H. C. Zhang, Q. Zhang, and T. J. Cui, "Efficient conversion of surface-plasmon-like modes to spatial radiated modes," Appl. Phys. Lett. **106**(2), 021102 (2015).
27. H. F. Ma, X. P. Shen, Q. Cheng, W. X. Jiang, and T. J. Cui, "Broadband and high-efficiency conversion from guided waves to spoof surface plasmon polaritons," Laser Photonics Rev. **8**(1), 146–151 (2014).
28. B. Ng, J. Wu, S. M. Hanham, A. I. Fernándezu-Domínguez, N. Klein, Y. F. Liew, M. B. Breese, M. Hong, and S. A. Maier, "Spoof plasmon surfaces: a novel platform for THz sensing," Adv. Opt. Mater. **1**(8), 543–548 (2013).
29. Z. Liao, X. Shen, B. C. Pan, J. Zhao, Y. Luo, and T. J. Cui, "Combined system for efficient excitation and capture of LSP resonances and flexible control of SPP transmissions," ACS Photonics **2**(6), 738–743 (2015).
30. N. Yu, Q. J. Wang, M. A. Kats, J. A. Fan, S. P. Khanna, L. Li, A. G. Davies, E. H. Linfield, and F. Capasso, "Designer spoof surface plasmon structures collimate terahertz laser beams," Nat. Mater. **9**(9), 730–735 (2010).
31. Y. Liu, H. Shi, C. Wang, C. Du, and X. Luo, "Multiple directional beaming effect of metallic subwavelength slit surrounded by periodically corrugated grooves," Opt. Express **16**(7), 4487–4493 (2008).
32. T. Jiang, L. Shen, J. J. Wu, T. J. Yang, Z. Ruan, and L. Ran, "Realization of tightly confined channel plasmon polaritons at low frequencies," Appl. Phys. Lett. **99**(26), 261103 (2011).
33. W. Zhu, A. Agrawal, and A. Nahata, "Planar plasmonic terahertz guided-wave devices," Opt. Express **16**(9), 6216–6226 (2008).
34. A. I. Fernández-Domínguez, E. Moreno, L. Martin-Moreno, and F. J. Garcia-Vidal, "Guiding terahertz waves along subwavelength channels," Phys. Rev. B **79**(23), 233104 (2009).
35. K. J. Kim, J. E. Kim, H. Y. Park, Y. H. Lee, S. H. Kim, S. G. Lee, and C. S. Kee, "Propagation of spoof surface plasmon on metallic square lattice: bending and splitting of self-collimated beams," Opt. Express **22**(4), 4050–4058 (2014).
36. A. Mekis, J. C. Chen, I. Kurland, S. Fan, P. R. Villeneuve, and J. D. Joannopoulos, "High transmission through sharp bends in photonic crystal waveguides," Phys. Rev. Lett. **77**(18), 3787–3790 (1996).
37. C. L. C. Smith, N. Stenger, A. Kristensen, N. A. Mortensen, and S. I. Bozhevolnyi, "Gap and channeled plasmons in tapered grooves: a review," Nanoscale **7**(21), 9355–9386 (2015).

1. Introduction

At optical frequencies, surface electromagnetic waves can sustain at the interface between noble metals and air, due to the interaction between surface-charge oscillation and the electromagnetic (EM) fields, which is the so-called surface plasmon polaritons (SPPs) [1]. One of the most important properties of SPPs is the confinement of light in subwavelength scale, which is promising for various applications, such as biosensing [2], photonic circuits [3, 4], surface-enhanced Raman scattering [5, 6], photovoltaics [7], nonlinear optics [8], broadband light localization [9–13] etc. Extending the concepts of highly localized waveguiding to lower frequencies, such as far-infrared, terahertz and microwave regime, would be of great advantage to building compact components for integrated circuits. However, at frequencies far from the intrinsic plasma frequency, the noble metals behave like perfect electric conductors, which can only support surface wave with weak confinement and

#241242 Received 18 May 2015; revised 29 Jun 2015; accepted 13 Jul 2015; published 15 Jul 2015

short propagation distance. In 2004, Pendry et al. suggested that metamaterial structures such as square hole lattices cut into the surface of a perfect electric conductor (PEC) can support bound electromagnetic waves that mimic the dispersion behavior of the SPPs in the optical range [14]. After that, different kinds of structured PEC surfaces, such as the one-dimensional subwavelength corrugations [15, 16], dominos [17, 18], corrugated metal wires [19, 20], complementary split-ring resonator metal films [21], corrugated metal films [22–27], etc, have been proposed to support spoof SPPs, showing potential applications in sensing [28, 29], laser beams [30], imaging, and directive emission [31]. In particular, spoof SPPs open the possibility of realizing compact waveguiding and focusing devices [32] operating at low frequencies. At the sub-wavelength scale, guiding electromagnetic waves through sharp bends in a plane with high efficiency is vital for the miniaturization of integrated circuits. Previous designs normally rely on moderate curved bends exceeding one-wavelength size to steer light gradually and in an adiabatic fashion [18, 32, 33], or employ a vertical structure to confine the modes around the tight corner [34, 35]. Thus, most of the spoof SPP bend devices are either of large volume or with a wavelength-comparable thickness. Achieving highly efficient transmission of spoof SPPs around ultrathin sharp bends remains a great challenge.

In this Letter, we present a promising route to guiding EM waves around 90-degree sharp corners in subwavelength scale using four-fold rotational symmetric planar structures. We show that the dispersion relation of spoof SPPs can be engineered at will by appropriate tuning of the geometrical parameters of the structures. The surface waves are demonstrated to propagate on a planar structured waveguides with a thickness of only 0.4 mm (relative to a wavelength of around 150 mm) over a broad frequency band in microwave spectrum. The high transmission efficiency is achieved by enhancing the confinement of spoof SPPs to suppress the scattering and reducing the reflection at the bend corner with proper design. To further understand and demonstrate the validity of our design, a one-dimensional scattering theory model is employed to verify the transmission properties of the waveguide bends with different arrangements. High transmission with a maximum of almost 100% is observed at several frequencies for 90-degree sharp bends, and a transmission of no less than 85% is achieved over a bandwidth of 2.1 GHz.

2. Theory and unit cell design

We first analyze the main reasons of the bending loss for spoof SPPs. The first reason is that the propagating spoof SPP modes couple with the radiation modes surrounding the bend region, resulting from the weak confinement of surface waves. This problem may be solved by improving the light confinement, which can be achieved through enlarging the momentum k of the spoof SPP relative to the k_0 of free-space radiation, *i.e.* increasing the deviation of the dispersion curve from the light line so that $(k-k_0)R \gg 1$ where R is the bend radius. Due to the mismatch between spoof SPP modes and radiation modes, only a modest energy fraction of the spoof SPPs is radiated into the surrounding space. The second reason, which is also the main reason that causes the bending loss, is the back reflection associated with the modes mismatch between spoof SPP propagating along the straight waveguide and that along the bends. This is a common problem for most of the bend waveguide systems. Here, to solve this problem, we design a structure with four-fold rotational symmetry for guiding spoof SPP modes. Besides, with proper design the mismatch of the momenta of spoof SPPs in the straight and bent structures are minimized to increase the transmission at the corner.

#241242 Received 18 May 2015; revised 29 Jun 2015; accepted 13 Jul 2015; published 15 Jul 2015

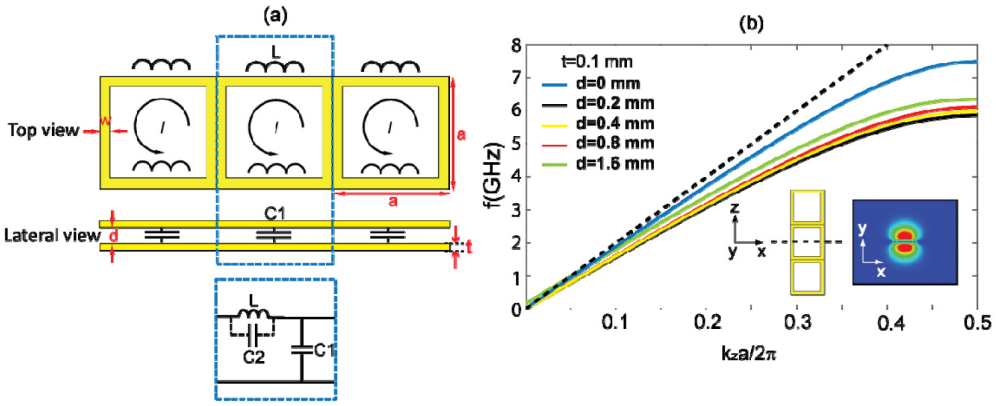

Fig. 1. (a) Schematic of the closed ring (CR) structure waveguide and the corresponding circuit model; (b) dispersion relation for the spoof SPPs propagating on the monolayer (the black line) CR waveguide and double-layer CR waveguides with different values of distance between two layers. Geometric parameters of a = 15 mm, w = 0.5 mm and t = 0.1 mm are fixed for all curves. The inset shows the normal electric field distribution of xy plane at $k_z = 0.45(2\pi/a)$.

Let us start by considering a very simple case with four-fold rotational symmetry, a closed-ring (CR) structure as shown in Fig. 1(a). The electromagnetic property of the CR is controlled by the geometry parameters, *i.e.*, period a, metal line width w, and metal thickness t. When imposing electromagnetic waves on a chain of such structures, a current loop will be induced on every metal ring. Thus, it is easy to get its equivalent circuit model, where we can obtain the spoof surface plasma frequency, $1/\sqrt{LC_2}$. The dispersion property of the CR spoof SPPs can be numerically calculated from an electromagnetic eigenvalue problem (We employ the commercial software CST Microwave Studio). Here, we set a = 15 mm, w = 0.5 mm and t = 0.1 mm, and the corresponding dispersion relation is depicted by the black curve in Fig. 1(b), which has the generic shape of a SPP at optical frequencies. However, the curve is very close to the light line [the black dashed line in Fig. 1(b)], because the capacitor induced by the metal ring is too small. To increase the wave vector of the spoof SPP mode, we introduce another capacitor, C_1, as shown in the circuit model in Fig. 1(a), by adding one more layer of CR chain (see the lateral view). Thus, the spoof surface plasma frequency becomes $1/\sqrt{L(C_1+C_2)}$. In our case, when the distance between two CR layers is d = 0.2 mm, the plasma frequency shifts from 7.5 GHz to around 6 GHz. It is interesting to see that when enlarging d, the dispersion is slightly shifted towards the light line. And when d goes to infinity, C_1 becomes zero, and the dispersion curve naturally converges to the one-layer case. The inset in Fig. 1(b) shows the normal component E_z of the electric field distribution in the xy plane at $k_z = 0.45(2\pi/a)$. As we can see, the gap between two layers can guide the EM waves along z direction, which tend to leak from the waveguide along x and y directions, but are confined by the ring structure and behave as evanescent waves.

#241242 Received 18 May 2015; revised 29 Jun 2015; accepted 13 Jul 2015; published 15 Jul 2015

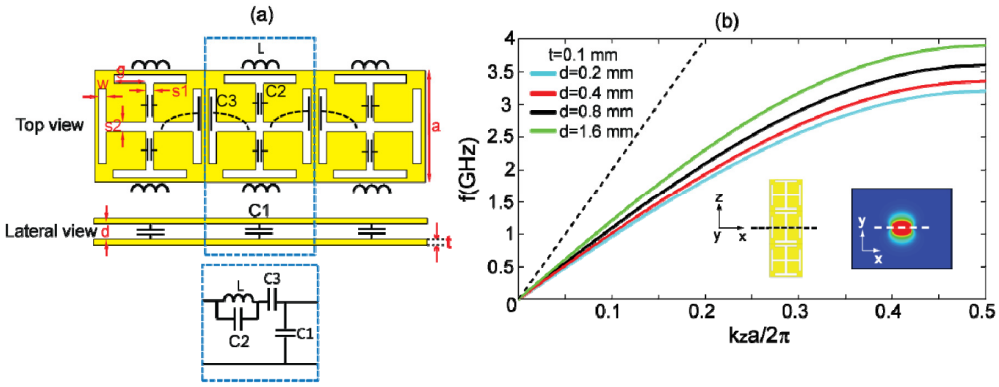

Fig. 2. (a) Schematic of the crossed H (CH) structure waveguide and the corresponding circuit model; (b) dispersion relation for the spoof SPPs propagating on the double-layer CH waveguides with different values of distance between two layers. Geometric parameters of a = 15 mm, w = 0.5 mm, g = 5.5 mm, $s1$ = $s2$ = 1 mm, and t = 0.1 mm are fixed for all curves. The inset shows the normal electric field distribution of xy plane at $k_z = 0.45(2\pi / a)$.

To further increase the momentum of the spoof SPPs, we enlarge the capacitor C_2, by adding a crossed-H shaped structure on each layer, see Fig. 2(a). In addition, this structure also introduces a mutual capacitor, C_3, between each neighboring unit cell. The corresponding equivalent circuit model is shown in the right-hand side of Fig. 2(a) and the spoof surface plasma frequency is accordingly changed to $1/\sqrt{L(C_2C_3 + C_1(C_2 + C_3)/(C_1 + C_3))}$. Here, we set a = 15 mm, w = 0.5 mm, g = 5.5 mm, $s1$ = $s2$ = 1 mm, t = 0.1 mm, and d = 0.2 mm, and consequently the spoof surface plasma frequency is decreased to 3.25 GHz. This new structure is still sensitive to d, and in Fig. 2(b), we show the dispersion relations in terms of different d. Similar to the previous case, the distance between the light line and the dispersion curve of CH spoof SPPs has an inverse relationship with d. The inset in Fig. 2(b) shows the normal component E_z of the electric field distribution in the xy plane at $k_z = 0.45(2\pi / a)$. It has a similar pattern to that of the CR spoof SPPs, but with stronger confinement along both x and y directions. Therefore, in what follows, we utilize this structure to realize transmission of spoof SPPs through sharp bends.

3. Simulations and models

To investigate the performance of our design, we show time-domain simulations (again employing CST) of the transmission of the spoof SPPs propagating through the bends. In the simulation, we use two ports to feed and receive the CH spoof SPPs at the ends of two arms of the 90-degree bent waveguide. As the ports are well coupled with the CH spoof SPPs, the ports can also work as probes to detect the amplitude of the signal. The feed port creates a pulse with Gaussian envelop in time. By using a sizable computational cell (64 unit cells for each arm in our case), we can distinguish and separate the different pulses, such as the first pulses reflected by and transmitted through the bend, which can be Fourier transformed to obtain the frequency-dependent transmission coefficient. We note that the radiation loss of the CH spoof SPPs in our cases is very small, which can be neglected when calculating the transmission. The numerically simulated transmission coefficient for the 90-degree bent waveguide with zero radius of curvature is given as the red solid line in the left panel of Fig. 3(a), where the transmission of above 90% can be observed from in a frequency range of 0-1.2 GHz. The inset shows the geometry of the bent waveguide considered in the simulation, and the E_z field distributions at 2 GHz is shown in the right panel. Due to the mismatch between the port and the CH spoof SPP, there are some reflections at the feeding port. One

#241242 Received 18 May 2015; revised 29 Jun 2015; accepted 13 Jul 2015; published 15 Jul 2015

may notice the phase change in and out of the CH spoof SPP waveguide. This is consistent with the electric field distribution shown in the inset of Fig. 2(b), where the phase various along the cut plane z = 1 mm (as indicated by the white dash line).

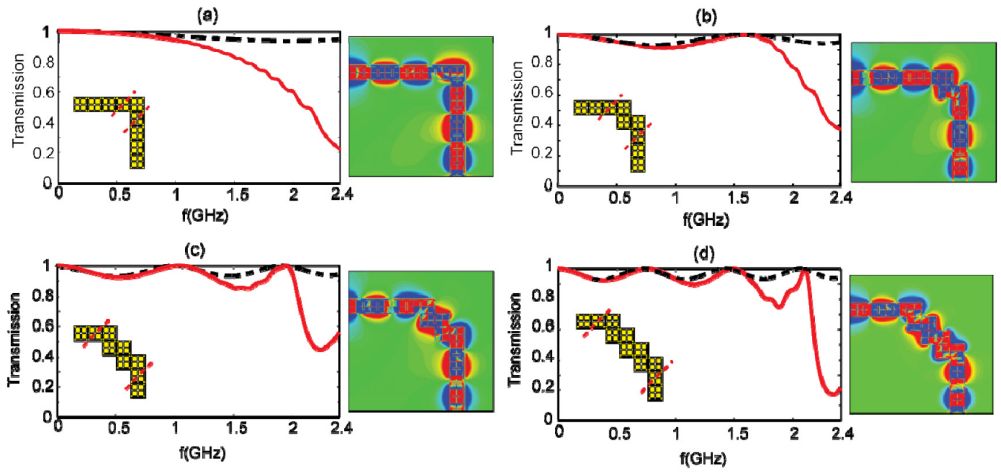

Fig. 3. Transmission coefficients and corresponding E_z field distributions (z = 1 mm) at 2 GHz for sharp CH spoof SPP waveguide bends with different geometries. The red solid transmission curves are numerically simulated results, while the black dash lines are calculated results obtained with the scattering model.

Normally, the bending loss for traditional waveguides is difficult to describe analytically because the radiative behaviors at the waveguide bending are very complicated. However, in our design, the spoof plasmon waveguide structure can support electromagnetic modes at deep subwavelength scales, where the radiative loss is negligible. Hence, at the waveguide bending corner, the electromagnetic waves can just be reflected back or transmitted through, which is similar to a one dimensional scattering problem. This allows us to use a one-dimensional scattering model [36] to theoretically calculate the transmission coefficients of the bent waveguide, so that the transmission property can be further improved. . The wave vector in the straight waveguide is defined as $k_1(f)$ and that in the bending corner as $k_2(f)$, which are given in Fig. 4. In the scattering process the spoof SPP mode first propagates in the straight waveguide with the wave vector $k_1(f)$, and it is then coupled to the mode with wave vector $k_2(f)$ inside the bend and finally it is coupled to the mode with wave vector $k_1(f)$ in the output arm of the bent waveguide. Therefore, the effective refractive indices in the straight and bent parts of the waveguide can be obtained accordingly. According to the one-dimensional scattering model [36], the transmission coefficient of the bent waveguide can then be estimated from

$$T(f) = 1 - [1 + (\frac{2k_1(f)k_2(f)}{[k_1^2(f) - k_2^2(f)]\sin[k_2(f)L]})^2]^{-1} \quad (1)$$

where L *i*s the effective length of the bend, which describes the effective path of SPP waves in the bending region. Therefore, L is associated with the geometry and the physical length of the bend and is related with the period of the bending unit, $\sqrt{2}a$ [see inset in Fig. 4]. From Eq. (1), we find that the transmission coefficient can be engineered by changing L. This can be physically achieved by increasing the number of cells at the bending corner. Figure 3(b) shows a modified spoof-SPP waveguide bend designed to improve the transmission property, where the bending corner is composed of two unit cells. In this way, we create a Fabry-Perot cavity with a length L. To obtain the value of L in the scattering model, we varied its value

#241242 Received 18 May 2015; revised 29 Jun 2015; accepted 13 Jul 2015; published 15 Jul 2015

and compared the scattering model based transmission coefficients with the simulated ones to make the 100% transmission point matched in both simulated and calculated methods. Compared with the original bending in Fig. 3(a), the modified bending shows an oscillation in the transmission, and the bandwidth for high transmission is increased. By further increasing the effective bend length L (adding multiples of $\sqrt{2}a$), we increase the effective length of the cavity, thereby allowing for multiple resonances where 100% transmission can be achieved. As shown in Figs. 3(c) and 3(d), the theoretical calculations (black dashed lines) agree with the numerical simulations (red solid lines) in predicting the general tendency of the transmission spectrums and the frequencies where 100% transmission occurs. Both of the calculated and simulated results confirm that the bandwidth broadens and more transmission peaks appear as more bending cells are added to the corner of the CH spoof SPP bends. For example, for the structure shown in Fig. 3(c), high transmission with a maximum of almost 100% is observed at 1.1 GHz and 1.95 GHz, and a transmission of no less than 85% is achieved over a bandwidth of 2.1 GHz. The field pattern of propagating modes at 2 GHz is given in the right panel. We note that the spoof SPP mode is strongly confined around the waveguide with negligible radiation into the surrounding space, and travels smoothly around the bend even for a radius on the order of the wavelength.

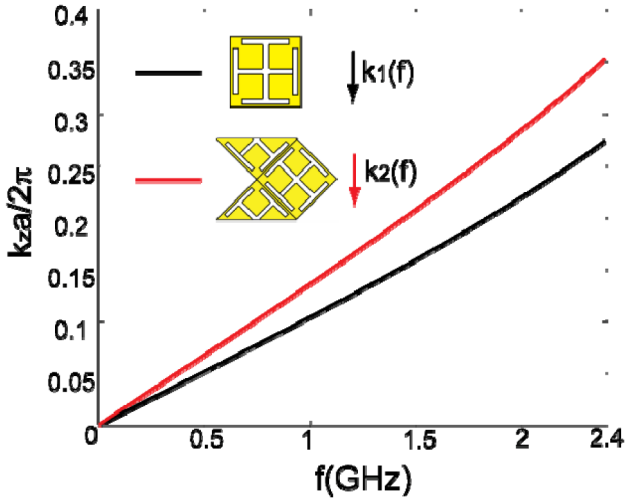

Fig. 4. Dispersion relations for spoof SPP modes in straight waveguide $k_1(f)$ (black line) and bending corner $k_2(f)$ (red line).

In conclusion, broadband ultrathin 90-degree planar sharp bends for spoof SPPs are designed in this work. In order to address the main causes for bend loses of spoof SPPs, *i.e.*, radiation loss and return loss, we design a four-fold rotationally symmetric structure to support high-momentum spoof SPPs. A one-dimensional scattering theory is employed to further understand and verify the transmission properties of our waveguide bend. Our design approach is not restricted to the specific structure we propose here and it can be applied to other guiding components built up on two dimensional metal surfaces (such as channel or wedge plasmon waveguides [37]). Our approach of realizing high transmission of spoof SPPs through sharp bends paves the way for miniature microwave and terahertz wave circuits.

Acknowledgments

The work is supported by Danish Research Council for Technology and Production Sciences (FTP grants #11-104559), National Natural Science Foundation of China under Grants No.61322501, and No.61275183, the National Program for Special Support of Top-Notch

#241242 Received 18 May 2015; revised 29 Jun 2015; accepted 13 Jul 2015; published 15 Jul 2015

Young Professionals, the Program for New Century Excellent Talents (NCET-12-0489) in University, the Fundamental Research Funds for the Central Universities, and the Innovation Joint Research Center for Cyber-Physical-Society System.

#241242 Received 18 May 2015; revised 29 Jun 2015; accepted 13 Jul 2015; published 15 Jul 2015